crystals

MDPI

Article

Influence of Temperature Field Distribution on the Growth of Aluminum Nitride Crystal by Simulation Technology

Shengtao Zhang [1], Wenbo Yuan [1], Guofeng Fan [2], Tie Li [3] and Lili Zhao [1,*]

[1] School of Chemistry and Chemical Engineering, Harbin Institute of Technology, Harbin 150001, China
[2] Soft-Impact China (Harbin), Ltd., Harbin 150028, China
[3] Harbin KY Semiconductor, Inc., Harbin 150028, China
* Correspondence: zhaolili@hit.edu.cn; Tel.: +86-188-4613-0714; Fax: +86-0451-84010483

Abstract: During the crystal growth process, the temperature distribution in the reactor plays a decisive role in crystal growth and directly affects the crystal growth rate. In this study, a numerical simulation method was used to model and study the temperature distribution in the PVT AlN crystal reactor. By adjusting the relative position of the heater and the crucible, different temperature field structures are obtained. The effect of different temperature gradients on the decisiveness of the crystal growth and the growth rate is explored and analyzed, and the best scheme is selected. With the help of simulation technology, a 52 mm diameter AlN crystal is successfully prepared with a certain thickness. The results prove the feasibility of the simulation scheme, which is supported by the existing experimental data.

Keywords: aluminum nitride crystal; numerical simulation; temperature field; temperature gradient; growth rate

Citation: Zhang, S.; Yuan, W.; Fan, G.; Li, T.; Zhao, L. Influence of Temperature Field Distribution on the Growth of Aluminum Nitride Crystal by Simulation Technology. *Crystals* **2022**, *12*, 1320. https://doi.org/10.3390/cryst12091320

Academic Editors: Evgeniy N. Mokhov, Yongsheng Han and Duncan H. Gregory

Received: 28 August 2022
Accepted: 13 September 2022
Published: 19 September 2022

1. Introduction

As representative of the wide bandgap semiconductor (WBG) materials, aluminum nitride (AlN) crystals have the advantages of high band gap width, high breakdown electric field, high thermal conductivity, high electron saturation rate, and high radiation resistance. They can be used as ideal substrates for GaN, AlGaN, and AlN epitaxial materials [1]. Compared to sapphire and SiC substrates, AlN has higher thermal matching and chemical compatibility with GaN, and the stress between the substrate and the epitaxial layer is smaller [2]. Therefore, using AlN crystals as a GaN epitaxial substrate can greatly reduce the defect density in a device, which will improve the performance of devices built using the crystals [3]. It has good application prospects in the preparation of high-temperature, high-frequency, high-power electronic devices, especially in blue-UV solid-state laser diodes, lasers, and GaN-based high-electron-mobility transistors (HEMT) devices and substrates for solar blind AlGaN ultraviolet detector devices [4]. The research and development of AlN crystals and the manufacture of various related devices will greatly promote the development of aerospace, defense, energy, and communications technologies.

The large-scale application of AlN is limited to the commercial production of high-quality AlN substrate materials. Thus, the preparation of high-quality, large-sized single crystals is of great significance. In particular, the application of AlN-based devices is still immature and has attracted worldwide attention [5]. Many international scientific research institutions have tried a variety of methods to prepare AlN crystals, mainly including the amonothermal method [6], flux/solution growth [7], hydride vapor phase epitaxy (HVPE) [8], and physical vapor transport (PVT) [9]. After decades of research, the PVT method is recognized as a more effective method for preparing high-quality, large-size AlN crystals and has gradually become the mainstream process for AlN single crystal preparation.

It is not easy to study the influence of temperature distribution on crystal growth, since the growth of AlN crystals using the PVT method requires a high temperature above 2200 °C in a closed space. Limited by testing methods, it is not possible to directly and accurately measure and characterize the temperature field distribution, flow field distribution, and crystal growth state in the furnace during crystal growth. On the other hand, the cost of growing AlN crystals via the PVT method is extremely high, and an experiment period lasts for more than 100 h, making it difficult to provide timely feedback on the growth process. To obtain the best growth process, we use STR VR-PVT AlN software as a numerical simulation tool to study deposition characteristics of AlN crystal growth, especially the temperature distribution between crystal and source. After the calculation converges, we use visualization module to make different physical parameters in the reactor becomes intuitive, which is helpful for understanding what happened inside the crucible during the AlN crystal growth process.

2. Experimental

The modeling equipment is the self-designed gas phase transmission system PVT AlN-180001 (referred to as the system), which is mainly composed of the furnace body and its internal thermal field, cooling water system, pressure holding system, and other parts. The whole operating system can be controlled by PLC automatic programs that set growth process parameters. For furnaces that have characteristics of symmetry along the radial direction, we established a 2D model to reduce unnecessary workload. Additionally, some insignificant details of the furnace were neglected, and the main blocks, such as the cylindrical furnace, heater, crucible, thermal insulation layer around the crucible, and thermal field structure in the crucible were reserved and in the spotlight. The general structure of the AlN single crystal growth furnace is as shown in Figure 1. The height of the furnace is 850 mm, the diameter of the bottom is 280 mm, and the thickness of the furnace wall is 10 mm. The furnace has a thin layer of tungsten-molybdenum insulation structure with a thickness 0.4 mm in a single layer. The heater has a height of 220 mm and is distributed around the crucible in a barrel shape. Other geometric parameters of the reactor are shown in Table 1. The seed crystal specifications used in the experiment are shown in Table 2. The thickness of AlN crystal on the tantalum sheet is greater than 1 mm. Limited by the preparation process of the seed crystal, some shallow cracks exist at the interface of SiC and AlN.

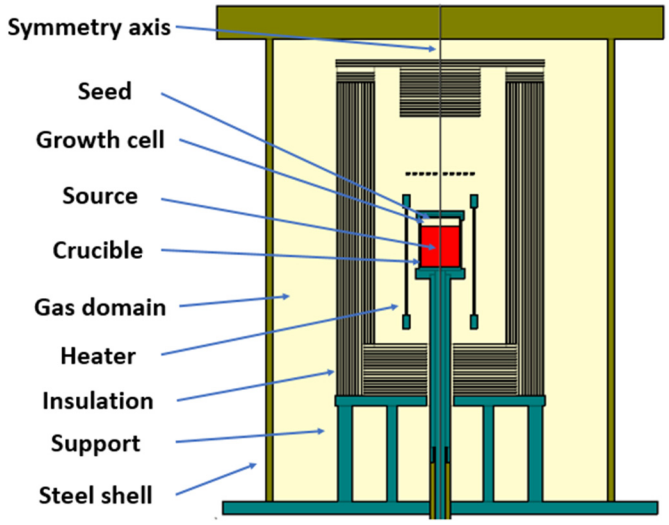

Figure 1. Structure of AlN single crystal growth furnace.

Table 1. The geometric dimensions of the PVT furnace.

Categories	Parameters
Furnace height (mm)	850
Furnace inner diameter (mm)	480
Thickness of furnace wall (mm)	10
Thickness of thin layer (mm)	0.4
Height of heater (mm)	220

Table 2. The specifications of AlN crystal seed.

Categories	Parameters
Diameter (mm)	850
Thickness (mm)	480
Diameter and thickness of Ta plate (mm)	$\varphi 60 \times 2$
Al surface	As grown
FWHM (arcsec)	400
Purity	Si~5%, C~5%

After the establishment of the physical model is completed, setting physical properties of the main materials is necessary before boundary condition definitions, which are found from public information and as shown in Table 3.

Table 3. Physical parameter of different materials.

Categories	W	Mo	AlN Crystal	Raw Materials
Thermal conductivity (W/(m K))	Polynomial (120.66, 1066 K)	Table (112, 1000 K)	Power-Exponential (107.1, 454 K)	-
Conductivity $((\Omega\ m)^{-1})$	1.9×10^7	1.99×10^7	1×10^{-10}	1
Density (kg/m^3)	19,350	10,220	3255	3255
Heat capacity (J/(kg K))	Polynomial (160.39, 1619 K)	Table (294, 1000 K)	Table (1167, 1000 K)	1000
Young's modulus (GPa)	411	329	-	-
Poisson's ratio	0.28	0.31	-	-
Surface emissivity	0.287	0.254	0.9	0.8

Before performing calculations, grids of object blocks must be obtained to map the physical space to the calculation space. To consider calculation accuracy and calculation efficiency simultaneously, triangular and hexagonal units are used in different parts according to block shapes to generate meshes, as shown in Figure 2. Meanwhile, different mesh densities are used in different regions. After generating grids in the calculation space and determine the coordinates of each grid node so as to describe the heat transfer and substance transfer problems of the crystal furnace with a mathematical model.

The simulation results are obtained through iterative calculations and the solutions of nonlinear partial differential equations. In software, the computations stop automatically as soon as the convergence is reached (i.e., the residuals become smaller than a given value) or the maximum number of iterations is performed. Table 4 shows how the residuals of the parameters, relaxation and iterations for different parts were set in this study. For different key parameters, different convergence requirements are adopted.

Table 4. Residuals parameter.

Categories	Residual	Relaxation	Iterations
Temperature	1×10^{-6}	0.97	5000
Species	1×10^{-5}	0.95	5000
Velocity	1×10^{-4}	0.95	5000

Table 4. *Cont.*

Categories	Residual	Relaxation	Iterations
Pressure	1×10^{-4}	0.95	5000
Static Pressure	1×10^{-5}	0.7	5000
Total Pressure	1×10^{-6}	0.7	5000
Growth Rate	1×10^{-4}	1	-
Thermal stress	1×10^{-5}	-	10,000

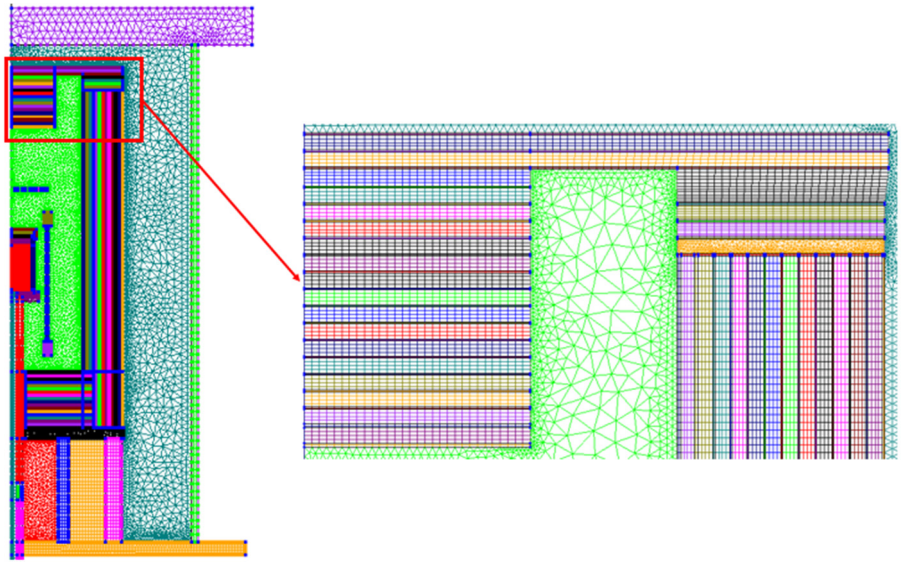

Figure 2. Adjusted model grid structure.

Temperature and temperature gradient inside the crucible is the principal condition of AlN crystal growth, which is significantly influenced by the relative position of the heating body and impossible to detect directly since the furnace is sealed and at high temperature inside during the working period. The heater of the system is made of metal tungsten, which is heated in a barrel shape around the crucible, and the heat radiation generated is a closed loop, in which the crucible receives different heat fluxes at different positions inside it. In this study, in order to determine the temperature field distribution of the appropriate relative position, the temperature at the top of crucible is set to 2060 °C and the crucible is heated at different positions, then the optimal position is determined according to the corresponding temperature gradient and growth curve. Meanwhile, the center line of the heating body and the center line of the crucible are used as the reference position 0, and the position of the crucible is unchanged to keep other conditions consistent.

3. Results and Discussion

3.1. Effect of Heating Body Position on Temperature Distribution

Figure 3 shows the effect of different positions of the heater on temperature distribution, and Figure 4 shows what the axial temperature gradient inside looks like. The high temperature zone in the crucible is located in the middle of the raw material zone when the heating body is at the center line of the crucible, as shown in Figure 3a, and in this case, the temperature range is from 2050 °C to 2127 °C. The high-temperature zone located in the middle of the raw material will produce a temperature gradient in the opposite direction, as shown in Figure 4a. In addition, the sublimated AlN vapor will condense on the surface and bottom surface of the raw material with lower temperature, which will affect the further volatilization of the raw material and reduce the raw material utilization rate. Figure 3b,c show that as the heating body moves upward, the overall temperature distribution inside the crucible drops significantly, and the high-temperature zone is located

above the raw material. Such a temperature distribution is not conducive to AlN crystal growth.

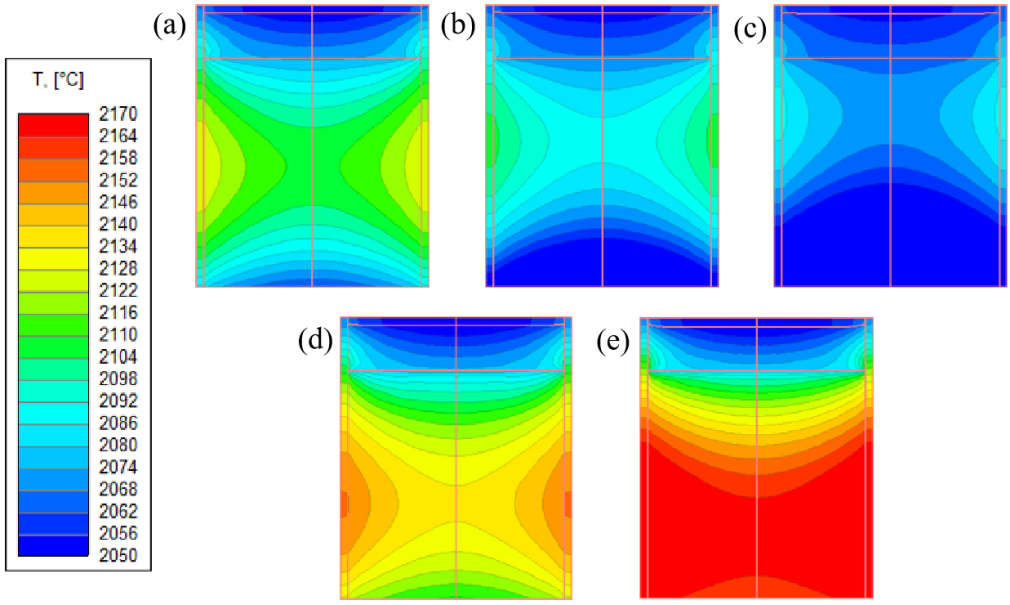

Figure 3. Effect of heating body position on temperature field distribution; (**a**) 0 mm, (**b**) 15 mm, (**c**) 30 mm, (**d**) −15 mm, and (**e**) −30 mm.

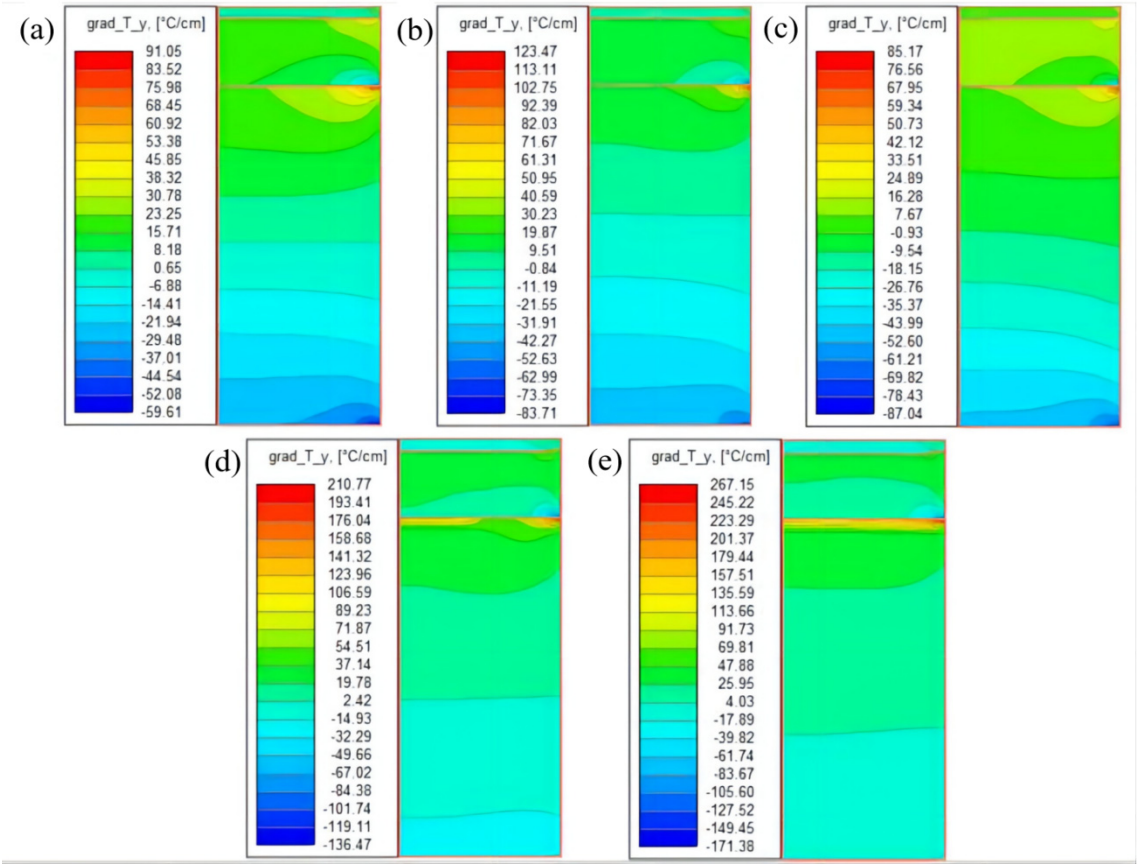

Figure 4. Effect of heating body position on axial temperature gradient; (**a**) 0 mm, (**b**) 15 mm, (**c**) 30 mm, (**d**) −15 mm, and (**e**) −30 mm.

When the high-temperature zone inside the crucible is above the raw material, a downward temperature gradient will occur, as shown in Figure 4b,c, and then the sublimated AlN vapor will be transferred to the low-temperature zone below the crucible and condenses on the raw material surface at the bottom. Secondly, the temperature in the center of AlN raw materials in Figure 3b is approximately 2080–2090 °C, which is 30 °C lower than in Figure 3a, leading to a small temperature gradient between crystal seed and raw materials. This means that the crystal growth rate will be significantly reduced. In contrast, Figure 3d,e show that when the heating body moves down, the overall temperature distribution inside the crucible rises. Meanwhile, the temperature in the center of the raw materials is approximately 2140 °C compared to 2110 °C in Figure 3a, 2090 in Figure 3b, 2080 °C in Figure 3c, and 2170 °C in Figure 3d. Figure 4d,e were obtained by changing the position by −30 mm. The downward shift of the high-temperature region creates a complete bottom-up temperature gradient with large numbers, which allows the sublimated AlN vapor to be transported upward from the bottom of the raw material to the surface of the AlN seed. In general, by changing the heater's position, the temperature difference between the raw material sublimation zone and the seed crystal crystallization zone can be controlled between 10–100 K, which is in good agreement with the literature [10]. The larger temperature gradient obtained ensures the higher growth rate of the crystal [11]. At the same time, the shapes of isotherms in Figure 3d,e are smooth and microconvex, which increases the stability of the crystal growth process and is conducive to obtaining a nearly flat microconvex crystal surface and improving the crystal quality.

3.2. Effect of Heating Body Position on Crystal Growth Rate

Reactive sublimation vapors are transferred to the low temperature zone for recrystallization and growth under the impetus of a temperature gradient and a concentration gradient. Distributions of gas phase components in the reaction chamber at different heater positions are as shown in Figure 5. It can be seen from the figure that when the position of the heating body gradually increases, the proportion of nitrogen components in the reaction chamber gradually changes from 0.97847–0.99443 and 0.98449–0.99437 to 0.988351–0.99657 with the upward movement of the high temperature zone, which indicates that with the upward movement of the heating body, the content of nitrogen components continues to increase, corresponding to the gradual decrease of aluminum components, which is similar to the decrease in aluminum components under high temperature conditions. The degradation of N/Al ratio during the reaction is consistent.

Figure 6 is the growth rate curve corresponding to different positions of the heater. When the heating body is in the center position of the crucible, the generated driving force causes the sublimated AlN raw material to be transported to the upper and lower ends of the crucible at the same time. Although the AlN crystal can grow at this time, the supersaturation is still very small, which will result in a lower growth rate of the AlN crystal, as shown by the black line. The heater moves upwards so that the high temperature region is above the raw material, resulting in the substrate temperature being equal to the surface temperature of the raw material. The resulting supersaturation is very small, the crystal is difficult to grow without a driving force or a small driving force, resulting in lower crystal growth rates as shown by the pink line and the green line. The heating body is moved down so that the high temperature zone is located at the bottom of the raw material, which overall increases the temperature distribution inside the crucible and further increases the temperature gradient from the surface of the raw material to the seed crystal. Therefore, the supersaturation of AlN crystal growth increases, which can increase the crystal growth rate, as shown by the blue red lines.

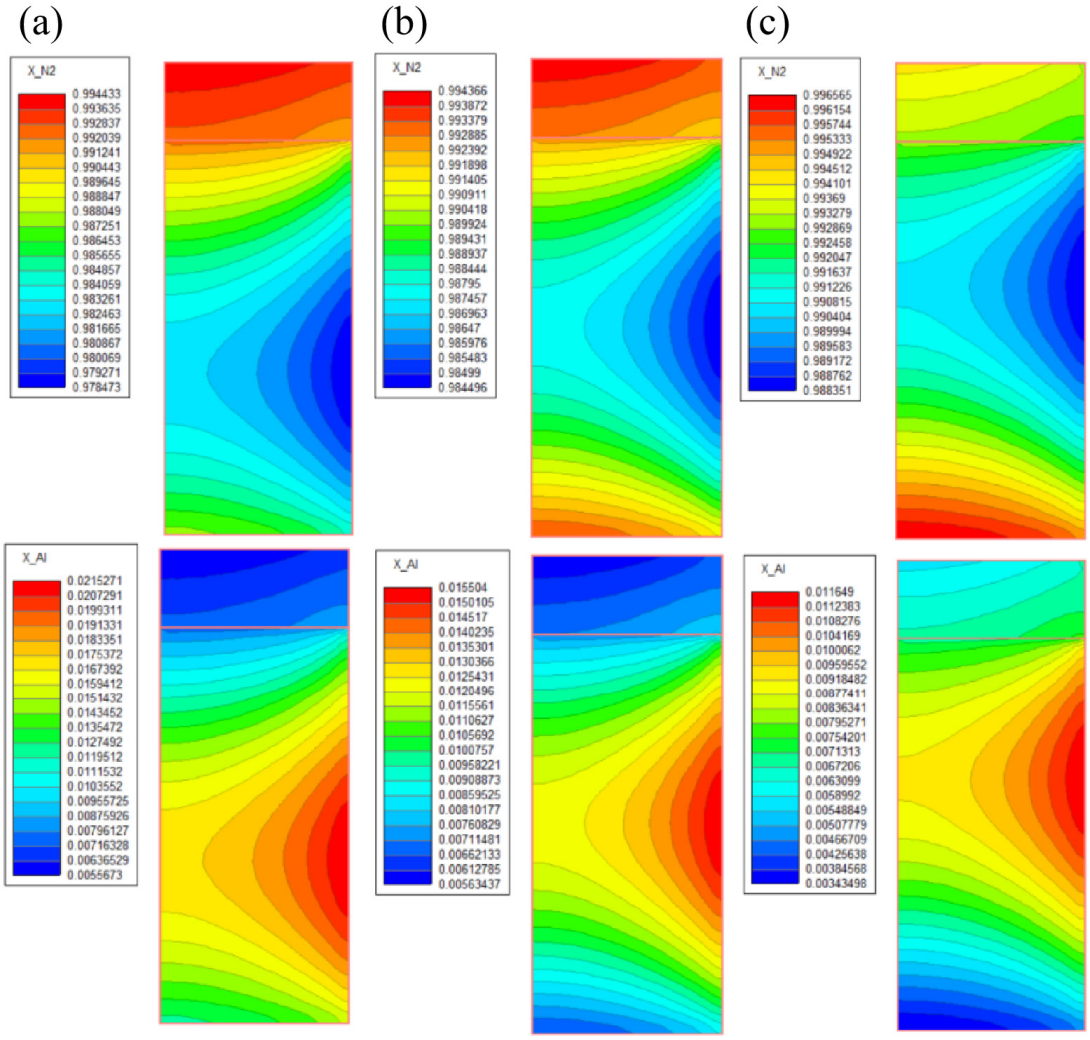

Figure 5. Species distribution (**a**) −15 mm; (**b**) 0 mm; (**c**) 15 mm.

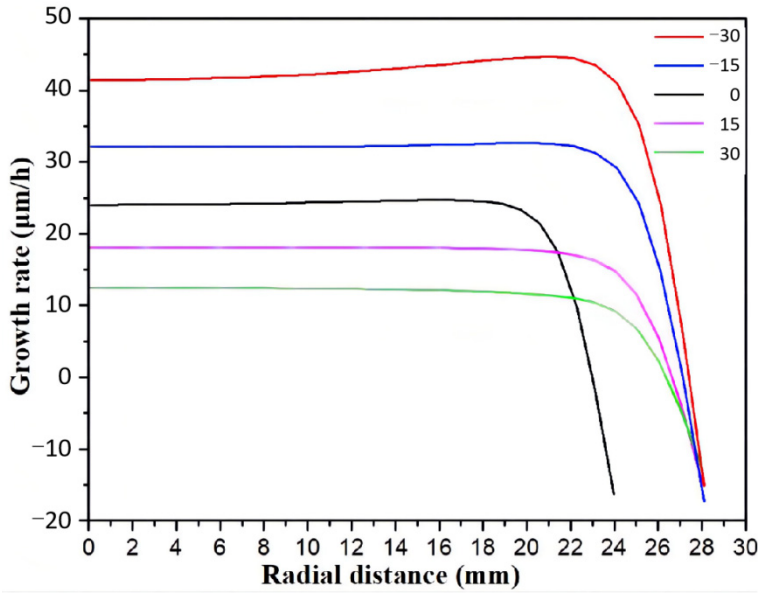

Figure 6. Effect of heating body position on crystal growth rate.

3.3. Characterization of AlN Single Crystal

Based on the simulation results, the heating body was lowered by 30 mm, and several tests were performed to grow crystals. AlN powder is pretreated at high temperature in nitrogen environments to reduce impurities, sintered into a polycrystalline state, and used as raw material for crystal growth. As shown in Figure 7, three crystals' surfaces are homogeneous and intact, no obvious cracks are observed, and the diameters are all above 52 mm. The thickness of the crystal verifies that a large temperature gradient is conducive to the axial growth of the crystal, and the contour of the crystal is in a micro convex shape, which is in good agreement with the simulation results. Meanwhile, crystal surfaces are not very smooth, which suggests that there are potential improvements to growth conditions.

Figure 7. Crystal morphology. (**a**) Sample 1; (**b**) Sample 2; (**c**) Sample 3.

Figure 8 shows the XRD diffraction patterns of the AlN wafers obtained through three sets of parallel experiments. The XRD pattern obtained shows a high-intensity diffraction peak at an angle of 36.04°, which can be matched with the (0002) diffraction peak in the standard card wurtzite AlN (PDF # 70-2545), and no impurity phase is detected. This shows that the crystal orientation of the obtained crystal is highly consistent and evenly distributed and grows along the direction of the c-axis polarity. The full widths at half-maximum (FWHM) of the three wafers are 273.6, 248.5, and 313.2 arcsec, respectively; these values are less than 400 arcsec. At −30 mm position, the temperature distribution characteristics of the thermal field reduce the possibility of radial growth, but maintain a good axial growth monocrystal degree and better inherit the quality of the seed crystal, and FWHMs below 400 arcsec also verify this. Meanwhile, there is no low-strength shoulder on either side of the main peak of the three test samples, which indicates that the crystal has no small angle grain boundary, and the looming medium- and high-strength shoulders indicate that there is a mosaic structure in the crystal, which will lead to the existence of stress. The symmetry on both sides of the main peak is high, which indicates that the crystallinity of the crystal with larger grain size is fairly good. In addition, a very low intensity diffraction peak was detected at an angle of 76.442, which corresponds to the (0004) direction. This may be due to some defects, such as thread dislocations, basal plane dislocations, and small angle grain boundaries—which require further specific study—existing in the crystal.

Raman spectroscopy detection is performed with backscatter geometry at room temperature. The Raman spectra of AlN wafers obtained from the three sets of parallel experiments are shown in Figure 9. The phonon modes observed in Raman spectroscopy follow the C_{6v} point group symmetry rule of the corresponding scattering structure. Three AlN wafers obtained almost the same Raman spectrum. Three phonon modes were observed at high intensity: E_2 (high) at 654.3 cm^{-1}, E_2 (low) at 246.8 cm^{-1}, and A_1 (LO) at 887.0 cm^{-1}. In particular, the wavenumber of the E_2 (high) mode, which is considered to be an indicator of the structural quality, is shifted to the lower wavenumber by 3.1 cm^{-1} from the stress-free AlN Raman frequency of the E_2 (high) mode (657.4 cm^{-1}) [12,13]. This indicates the presence of low tensile stress. The E_2 (high) modes' FWHM ranges are determined to be 2.88–2.91 cm^{-1}, which are superior to those of the AlN single crystal grown using both the self-nucleation technique (FWHM = 3 cm^{-1}) [14] and homoepitaxial/heteroepitaxial seeding technique (FWHM = 4–8 cm^{-1}) [15]. The above results mean that the grown

wafer has high structural quality with excellent uniformity and that there are no polytype inclusions inside the wafer.

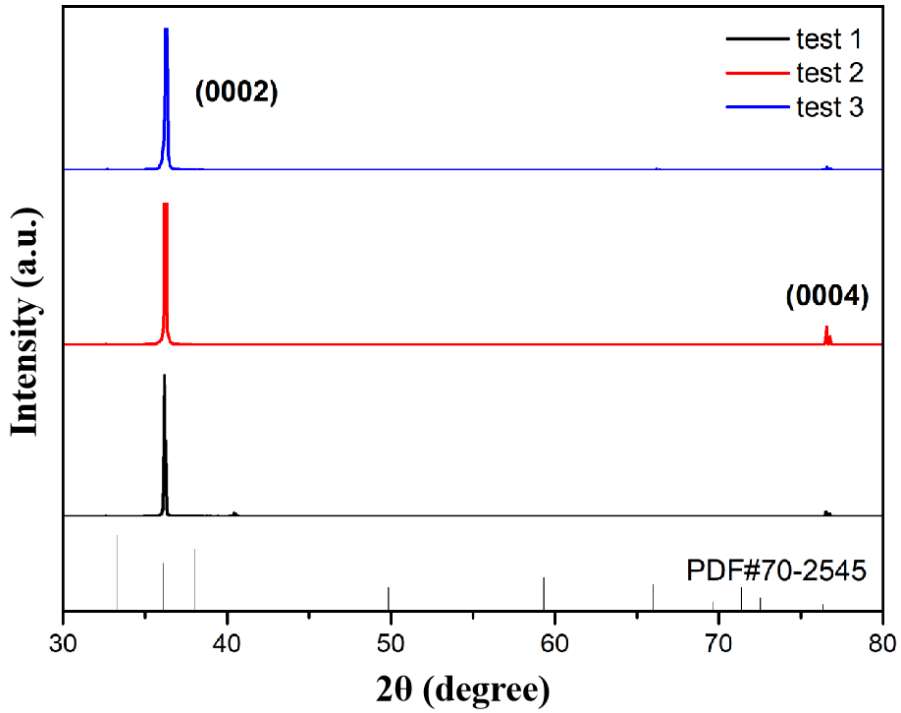

Figure 8. XRD diffraction pattern of AlN wafer.

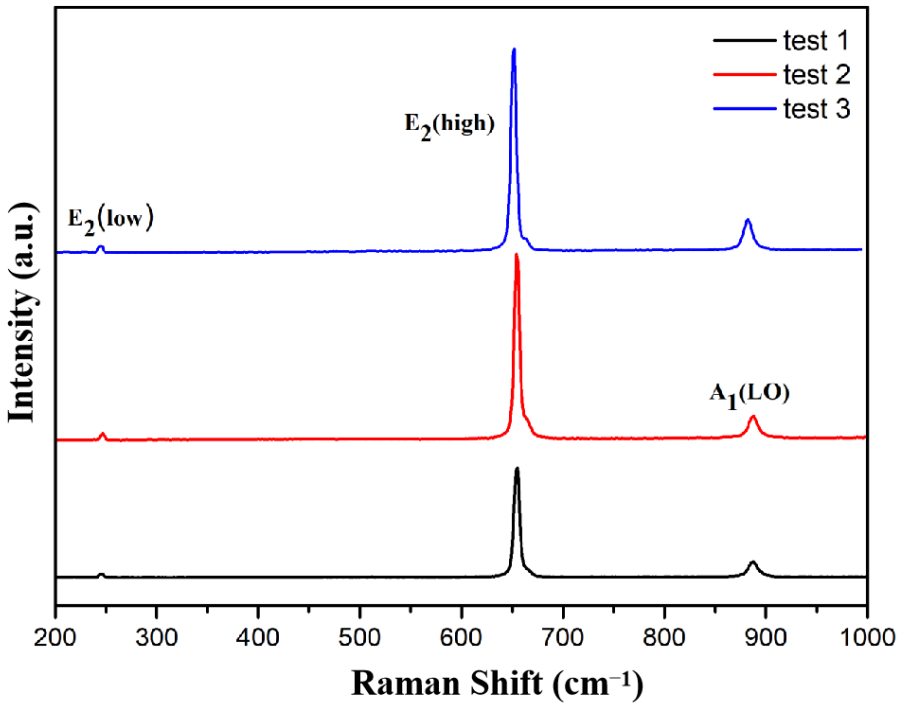

Figure 9. Raman spectrum of AlN wafer.

4. Conclusions

Under the same insulation structure, adjusting the relative position of the heater and the crucible can produce a significantly different temperature field gradient distribution, which in turn affects the supersaturation of the gas phase components on the seed crystal surface and the crystal growth rate. Moving the heater down will increase the temperature

gradient from the surface of the raw material to the seed crystal, increase the supersaturation of the crystal surface, and increase the crystal growth rate. When the heater is located 30 mm below the crucible, a temperature gradient from bottom to top is obtained. The temperature difference between the raw material and the substrate surface is 23.26 °C, while the axial temperature gradient is 29.79 °C/cm. In this condition, formed supersaturation can generate enough driving force to deposit and grow gaseous components uniformly on the surface of the seed crystal. Experiment shows the AlN grown by the simulation scheme is a single crystal with a highly uniform crystal orientation and uniform distribution. The grain size is large, and the crystallinity is high, with a high-quality structure, excellent uniformity, and lower thermal stress inside the crystal. However, there are some defects, such as thread dislocations, basal plane dislocations and small angle grain boundaries. These results show that the simulation method can provide significant guidance for the study of AlN single crystal preparation conditions.

Author Contributions: Conceptualization, S.Z.; methodology, S.Z. and W.Y.; software, G.F.; validation, G.F.; formal analysis, W.Y. and G.F.; investigation, T.L.; data curation, S.Z.; writing—original draft preparation, S.Z. and W.Y.; validation, G.F.; writing—review and editing, L.Z.; visualization, W.Y.; supervision, L.Z. and T.L.; project administration, T.L.; funding acquisition, L.Z. All authors have read and agreed to the published version of the manuscript.

Funding: This research was funded by [Major Scientific and Technological Achievements Transformation Projects of Heilongjiang Province of China] grant number [CG20A008], [Natural Science Foundation of Heilongjiang Province] grant number [JQ2019E003], [2021 Harbin Science and Technology Special Plan Project] grant number [2021ZSZZGH10]. The APC was funded by [Major Scientific and Technological Achievements Transformation Projects of Heilongjiang Province of China].

Institutional Review Board Statement: Not applicable.

Informed Consent Statement: Not applicable.

Acknowledgments: The authors thank Soft-Impact China (Harbin), Ltd. Harbin. for its support in simulation content.

Conflicts of Interest: The authors declare that they have no known competing financial interest or personal relationship that could have appeared to influence the work reported in this paper.

References

1. Grandusky, J.R.; Gibb, S.R.; Mendrick, M.C.; Moe, C.; Wraback, M.; Schowalter, L.J. High Output Power from 260 nm Pseudomorphic Ultraviolet Light-Emitting Diodes with Improved Thermal Performance. *Appl. Phys. Express* **2011**, *4*, 082101. [CrossRef]
2. Hirayama, H.; Yatabe, T.; Noguchi, N.; Ohashi, T.; Kamata, N. 231–261 nm AlGaN Deep-Ultraviolet Light-Emitting Diodes Fabricated on AlN Multilayer Buffers Grown by Ammonia Pulse-Flow Method on Sapphire. *Appl. Phys. Lett.* **2007**, *91*, 071901. [CrossRef]
3. Kneissl, M.; Yang, Z.; Teepe, M.; Knollenberg, C.; Schmidt, O.; Kiesel, P.; Johnson, N.M. Ultraviolet Semiconductor Laser Diodes on Bulk AlN. *J. Appl. Phys.* **2007**, *101*, 123103. [CrossRef]
4. Wunderer, T.; Chua, C.; Northrup, J.; Yang, Z.; Johnson, N.M.; Kneissl, M.; Garrett, G.A.; Shen, H.; Wraback, M.; Moody, B.; et al. Optically Pumped UV Lasers Grown on Bulk Al N Substrates. *Phys. Status Solidi* **2012**, *9*, 822–825. [CrossRef]
5. Radhakrishnan, S.R. Native Seeding and Silicon Doping in Bulk Growth of AlN Single Crystals by PVT Method. *Phys. Status Solidi* **2014**, *11*, 545–548. [CrossRef]
6. Satoh, I.; Arakawa, S.; Tanizaki, K.; Miyanaga, M.; Yamamoto, Y. Sublimation Growth of Nonpolar AlN Single Crystals and Defect Characterization. *Phys. Status Solidi* **2010**, *7*, 1767–1769. [CrossRef]
7. Zuo, S.; Wang, J.; Chen, X.; Jin, S.; Jiang, L.; Bao, H.; Sun, W.; Wang, W. Growth of AlN Single Crystals on 6H-SiC(0001) Substrates with Al N MOCVD Buffer Layer. *Cryst. Res. Technol.* **2012**, *47*, 139–144. [CrossRef]
8. Baker, T.; Mayo, A.; Veisi, Z.; Lu, P.; Schmitt, J. Hydride Vapor Phase Epitaxy of AlN Using a High Temperature Hot-wall Reactor. *J. Cryst. Growth* **2014**, *403*, 29–31. [CrossRef]
9. Hartmann, C.; Dittmar, A.; Wollweber, J.; Bickermann, M. Bulk AlN growth by physical vapour transport. *Semicond. Sci. Technol.* **2014**, *29*, 084002. [CrossRef]
10. Wu, H.-L.; Zheng, R.-S.; Yan, Z.; Li, M.-M.; Zheng, W. Effect of temperature distribution on growth habit of AlN crystal. *J. Shenzhen Univ. Sci. Eng.* **2012**, *6*, 471–580. [CrossRef]

11. Wang, G.; Zhang, L.; Wang, Y.; Shao, Y.; Chen, C.; Liu, G.; Wu, Y.; Hao, X. Effect of temperature gradient on AlN crystal growth by PVT method. *Cryst. Growth Des.* **2019**, *19*, 6736–6742. [CrossRef]
12. Kuball, M.; Hayes, J.M.; Shi, Y.; Edgar, J.H.; Prins, A.D.; van Uden, N.W.A.; Dunstan, D.J. Raman scattering studies on single-crystalline bulk AlN: Temperature and pressure dependence of the AlN phonon modes. *Crys. J. Growth* **2001**, *231*, 391–396. [CrossRef]
13. Davydov, V.Y.; Kitaev, Y.E.; Goncharuk, I.N.; Smirnov, A.N.; Graul, J.; Semchinova, O.; Uffmann, D.; Smirnov, M.B.; Mirgorodsky, A.P.; Evarestov, R.A. Phonon dispersion and Raman scattering in hexagonal GaN and AlN. *Phys. Rev. B* **1998**, *58*, 12899. [CrossRef]
14. Kuball, J.M.M.; Hayes, A.D.; Prins, N.W.A.; vanUden, D.J.; Dunstan, Y.; Shi, J.H. Raman scattering studies on single-crystalline bulk AlN under high pressures. *Appl. Phys. Lett.* **2001**, *78*, 724. [CrossRef]
15. Wang, Q.; Lei, D.; He, G.; Gong, J.; Huang, J.; Wu, J. Characterization of 60 mm AlN Single Crystal Wafers Grown by the Physical Vapor Transport Method. *Phys. Status Solidi* **2019**, *216*, 1900118. [CrossRef]